Midway Progress Report

on

INVESTIGATION OF THE STRUCTURE OF RADIATION DAMAGE IN LITHIUM DIFFUSED SILICON

1 January 1970 through 1 June 1970

Contract No. 952456

Principal Investigator:

John C. Corelli
Nuclear Science Department
Rensselaer Polytechnic Institute
Troy, New York 12181

Prepared for:

National Aeronautics and Space Administration
Jet Propulsion Laboratory
4800 Oak Grove Drive
Pasadena, California 91103

Midway Progress Report

on

INVESTIGATION OF THE STRUCTURE OF RADIATION DAMAGE IN LITHIUM DIFFUSED SILICON

1 January 1970 through 1 June 1970

Contract No. 952456

Principal Investigator:

John C. Corelli
Nuclear Science Department
Rensselaer Polytechnic Institute
Troy, New York 12181

Prepared for:

National Aeronautics and Space Administration
Jet Propulsion Laboratory
4800 Oak Grove Drive
Pasadena, California 91103

Midway Progress Report

on

INVESTIGATION OF THE STRUCTURE OF RADIATION DAMAGE IN LITHIUM-DIFFUSED SILICON

1 January 1970 through 1 June 1970

Contract No. 952456

Prepared for:

National Aeronautics and Space Administration
Jet Propulsion Laboratory
4800 Oak Grove Drive
Pasadena, California 91103

"This work was performed for the Jet Propulsion Laboratory, California Institute of Technology, as sponsored by the National Aeronautics and Space Administration under Contract NAS7-100"

Nuclear Engineering and Science Division
Rensselaer Polytechnic Institute
Troy, New York 12181

TABLE OF CONTENTS

ABSTRACT

A brief description is given of instrumentation and methods used in the study of radiation damage in lithium-diffused silicon in which infrared photoconductivity and infrared spectroscopy are used as the probes. The defects were induced in the material by 1.5 MeV electrons at 300°K. Also included is a detailed description of the cryostat to be used in cold temperature electron irradiations which permits both electrons of $<$ 3 MeV and light of 1 to 15 microns to irradiate the sample.

The main results are for infrared photoconductivity (PC) studies on irradiated samples. The PC spectrum was measured on one unirradiated Li-diffused sample containing 1.2×10^{16} lithium atoms/cm^3 in order to study background photoconductivity due to the lithium impurities. The result obtained is that the PC signal is 50 to 100 times smaller than for irradiated samples and additionally no single well defined energy level (or levels) dominates PC up to within 0.3eV of the conduction band. All samples studied which have $[Li] = 2 \times 10^{17}$, 6×10^{17}, and 9×10^{15}cm^{-3} exhibit sharp increases in resistivity after irradiation and after $\sim$ 100°C anneals. The dominant radiation-induced photoconductivity arises from levels at E_c-0.60, E_c-0.28, E_c-0.82, E_c-0.64, E_c-0.39, and E_c-0.23eV in the oxygen-rich material and at E_c-0.86, E_c-0.65, and E_c-0.34eV in oxygen-lean material. Both CG and FZ material exhibit photoconductivity due to levels (or a level) within about 0.20eV of the conduction band which we show is due to a defect containing at least one lithium atom. Defect energy levels due to the singly negative charge state of the divacancy are not observed. In all cases, the PC spectrum is dominated by fewer energy levels after subjecting the samples to 15 minutes at $\sim$100°C.

INTRODUCTION

The main effort of the research program during the time period 1 January 1970 through 1 October 1970 is aimed at the following.

a) Perform cold temperature (80°K) irradiation of Li-doped Si containing $\sim 10^{16} \frac{\text{lithium atoms}}{\text{cm}^3}$. The silicon samples are to be cut from two kinds of material i) crucible grown oxygen-rich $\gtrsim 10^{17}$ oxygen atoms/cm^3 and ii) floating zone oxygen-lean $\lesssim 10^{16}$ oxygen atoms/cm^3. The probes to be used to detect and characterize the defects are the infrared photoconductivity (PC) (with capability for studying the range 1 - 10 microns) and infrared spectroscopy (IR) (with capability for studying the range 1 - 20 microns).

b) Perform room temperature irradiations of Li-doped Si and examine the radiation induced extrinsic photoconductivity and effects of annealing. Where possible, correlate the energy levels which exhibit photoconductivity with thermally excited energy levels obtained by other workers in studies of the temperature dependence of carrier concentration.

A portion of the results included in this report were presented at the Third Annual Conference on "The Effects of Lithium Doping in Si Solar Cell Behavior", 27-28 April 1970, at the Jet Propulsion Laboratory.

The two most significant accomplishments of our program during the past six months have been an improvement of our method for measurement of infrared photoconductivity and preliminary testing of a cryostat to be used in our cold temperature irradiation studies of infrared photoconductivity and spectroscopy. The improvements in PC measurements consist of i) a better method of applying contacts to the sample which are ohmic and cause less noise generation, ii) purging the system to decrease CO_2 and water vapor absorption,

iii) careful electrical shielding of the system and iv) repair of wavelength drive so as to always have reproducible wavelength. The main significance of these improvements is that they enable us to make more accurate PC measurements and improve our signal to noise ratio. We present a detailed description of the cryostat in this report.

The level of the effort on this program is such that the work to be described in this report represents a 0.4 man year made up of the principal investigator, a graduate student, and one undergraduate student assistant, all on a part time basis.

EXPERIMENTAL METHODS

A) Samples and Optical Systems

In order to measure photoconductivity, it is necessary to make at least two electrical contacts to the silicon bar sample. In our experiments, the bar has nominal dimensions $\approx$ 2 x 5 x 20mm. Our previous samples were made by alloying gold doped with As to 0.1 atomic percent. We discovered that these contacts while quite suitable for our work in past years (for As-, P-, and Sb-doped Si) were unsatisfactory in studies on irradiated Li-doped Si since the contacts rectified after irradiation. We attribute this deterioration to the fact that our gold contained too little arsenic (0.1%) and that the negative carriers probably were depleted in the irradiation by the Li thus causing rectification at 78°K. Through the kind offices of Dr. G. Brucker and Mr. D. Leibowitz of RCA Laboratories we were informed of an alloying technique in which gold doped to 1 or 2 atomic percent Sb gave good ohmic contacts at 80°K even after irradiation of Li-doped Si samples containing Li to concentrations of $\gtrsim 10^{15}cm^{-3}$. The contacts made following the techniques of Brucker and Leibowitz retained their ohmic character even after irradiation and are the contacts we are currently using on our samples.

The infrared spectra are measured using Perkin-Elmer models 621 and 112 spectrometers to cover the wavelength region from 1 to 50 microns. A Perkin-Elmer model 98 monochromator which is enclosed in an airtight aluminum box is used in the photoconductivity measurements. Recently, we made modifications on the box which enables us to better purge our system of CO_2 and H_2O vapors which give rise to absorption bands normally found in the 1.5 to 7 micron wavelength region. We have also re-aligned the infrared monochromator optics in the model 98 in order to achieve easily reproducible wavelengths using the fiduciary marker on the monochromator.

B) Irradiation Cryostat for Photoconductivity and Infrared Spectroscopy

The basic cryostat used in our work is an Andonian Associates liquid helium cryostat model MHD-3L-30N equipped with a modified option 24 tail piece. The modified cryostat was used on previous work not associated with the task of the present contract. In Figure 1 we show the details of the tail piece of the cryostat and how the light is admitted into the cryostat and allowed to pass through the sample. The NaCl windows are at room temperature and the space between the AgCl window (5) (indium O-rings) and NaCl window (6) (neoprene O-rings) is evacuated to 10^{-6}-10^{-7}mm Hg. The AgCl window is normally in a cold environment in the space immediately surrounding the sample. Infrared light from 1 to about 16 microns can pass through the window system shown in Figure 1. The coolant (either liquid nitrogen or liguid helium) passes through the capillary collant transfer tube from the reservoir to the sample chamber volume. The heaters (7) are energized to vaporize the liquid so that during irradiation the electrons ($\sim$ 2.5-3 MeV) lose relatively little energy $<$ 200 keV in passing through the gas prior to striking the sample. The thermocouple 8 is used to sense the temperature, either a copper-constantan or gold (1%Fe) -copper thermo element is utilized above and below 80^{o}K, respectively.

In Figure 2 we show how the electron beam enters the cryostat tail piece 90^{o} relative to the infrared light beam direction shown in Figure 1. The electrons first pass through a 0.0005" Kapton Polymide film* (1) sealed with neoprene "O-rings". The electrons then pass through a cold window 0.003" thick aluminum (2) before striking the sample (5). Electrons are stopped in the cryostat and by a ½" thick lead sheet placed outside the cryostat after window (4). The sample is mounted is such a way that it can be freely rotated in the sample holder tube through 360°.

The electron beam is supplied by a 3 MeV van de Graff which is mounted in a vertical direction. The beam is bent through 90° by means of a magnet system so that the incident electrons move in a horizontal direction during irradiation of the sample.

*Available from E. I. Dupont De Nemours & Co. (Inc.)
Film Department, Wilmington, Delaware 19898

RESULTS AND DISCUSSION

In all results to be presented the measurement of the radiation-induced extrinsic photoconductivity by 1.5 MeV electrons was made at 78°K on samples several days after cessation of the bombardment. The sample temperature during bombardment was kept at $\lesssim$ 30°C. Consequently, all defects we are observing are those having long term ($\sim$ days) stability at 0°C.

For a point of reference (and comparison) we have shown in Figure 3 extrinsic photoconductivity due to impurities for an unirradiated silicon sample Li-diffused to 1.2 x 10^{16} lithium atoms/cm^3. In general, unirradiated Li-doped Si exhibits PC 50 to 100 times smaller than irradiated material. Measurements on unirradiated material of varying Li content are now being made and were not made on some of the samples since we were rushed for time and wanted to perform our irradiations with dispatch. We do not consider it important to examine every sample before irradiation due to low inherrent extrinsic PC from unirradiated Si. After decrease of the intrinsic photoconductivity at $\approx$ 1eV we still observe a fairly significant signal out to about 0.3eV measured with respect to the bottom of the conduction band. In general this photoconductivity signal is 50 - 100 times smaller than the signal induced in samples exposed to radiation. Therefore it is reasonable to expect that "background" extrinsic photoconductivity due to impurities is small relative to the PC of defects in irradiated samples. Another feature of the background photoconductivity is that no single well defined energy level dominates in the process. Note the PC is plotted on an arbitrary scale and can not be compared sample to sample.

A word of explanation telling how we determine that the level is measured from the conduction band edge is in order. Initially (i.e., before irradiation) we have mainly electron carriers in the n-type sample. After irradiation the carriers are trapped on defects giving rise to localized energy states below the Fermi level. The Fermi level is roughly experimentally determined by the energy where the PC signal cuts off. We assume there are no empty states below the Fermi level which would produce hole excitation in the sample. Therefore our energy levels are quoted relative to the bottom of the conduction band and involve electron excitation; since we further assume that empty states above the Fermi level have very low probability for capturing an electron from the valence band and causing PC by hole conduction in the valence band.

In Figure 4 we show the PC spectrum for a CG sample (JPL-11) Li doped to $9 \times 10^{16} cm^{-3}$ after it received a fluence of 6×10^{17} e/cm^2. The error bars are shown for the points at the lower energy, i.e., 0.24 to 0.35eV, whereas for all other points the error bars lie <u>within the point that is plotted</u>. We also show on the figure our <u>worst energy</u> resolution, and for most of the points the energy resolution is actually higher. In all subsequent spectra to be presented, the same presentation of experimental errors and energy resolution will be followed. After a 15 minute anneal at 100°C, the sample given in Figure 4 JPL-11 exhibits the photoconductivity spectrum shown in Figure 5. One feature of the spectrum after annealing is that the photoconductivity appears to be dominated by two energy levels, one at E_c-0.28eV and another at E_c-0.60eV and a rather abrupt increase in PC at about 0.24eV. More will be said of the abrupt increase in PC later as it has appeared in other samples. For all results to be given we adopt the convention that the energy level position is defined as that value where we observe the onset of ionization of the level. In many cases as for example Figure 4, the energy levels are seemingly masked and it is very difficult to pinpoint or even discern clear energy levels. Although we risk the chance of error in quoting energy levels for results such as in Figure 4, the fact that the "structure" lies outside our experimental error prompts us to take note of these breaks and assign energy levels to them. However, such energy levels may not be as important in associating them with specific defects as are the well defined energy levels in Figure 5 which we observed after heating sample (100°C).

The PC spectrum of a float zone sample Li-diffused to 9×10^{15} lithium atoms/cm^3 after irradiation to a fluence of $2 \times 10^{17} e/cm^2$ is shown in Figure 6 before annealing. After a 15 minute anneal at 110°C, this sample yielded the PC spectrum shown in Figure 7. Here again, note that before anneal we observe more structure in the spectrum, whereas after the heat treatment we can see that the PC is dominated by levels at E_c-0.86, E_c-0.65, and E_c-0.34eV, and again we observe a dramatic increase in the PC for energies below $\approx$ 0.24eV. In our experiments, thus far, we used a LiF prism as the dispersing medium and we can not go to wavelengths greater than $\approx$ 6 microns. This is the reason no measurements below 0.22eV are shown in Figures 5 and 7. Measurements beyond 5 - 6 microns will be made in the near future using a CaF_2 prism as the dispersing medium (transmits to $\approx$ 9 microns). A careful wavelength calibration of the CaF_2 will be required since we have not had this prism in the monochromator in our previous work.

Photoconductivity exhibited by a crucible grown sample Li-diffused to 2×10^{17} lithium atoms/cm^3 is shown in Figure 8. This relatively high lithium concentration and fluence gives rise to an extrinsic PC which appears to be dominated by three levels with additional evidence for a level closer than 0.23eV to the conduction band.

The abrupt increase in PC (Figures 5 and 7) for energies below 0.24eV has not been observed by us[1] in any of our previous work on P-doped silicon containing both high and low oxygen concentrations. We[2] have also recently completed extensive photoconductivity measurements on 1.5 MeV electron-irradiated non-lithium containing P-doped silicon with 15 minute anneals in 15°C steps from 90°C up to 200°C and have not observed the sudden increase in PC below 0.24eV. These findings strongly suggest the presence of a level within about 0.10 to 0.20eV below the bottom of the conduction band and this level may arise from a defect which must contain at least one lithium atom as one of the constituents. This conclusion is consistent with the recent findings of Brucker et.al., (3) of the RCA Laboratory who observed an energy level at E_c-0.14eV after $\approx$ 1 MeV electron bombardment (at 95°K) of F.Z. Si Li-diffused to 5 x $10^{15}cm^{-3}$ and in another sample Li-diffused to 1.8 x $10^{14}cm^{-3}$. Additional evidence for a radiation-produced defect energy level at E_c-0.13eV associated with Li atoms has been reported by Stannard(4). Both Brucker et. al,(3) and Stannard(4) use temperature dependence of carrier concentration to determine the energy level position. In their case(3,4) the carrier is <u>thermally excited</u> from the energy level into the conduction band, whereas in the present PC measurements the carrier is <u>optically excited</u> from the level. However, one additional point of consistency between the present PC results and the carrier concentration measurements of Brucker et.al.(3) and Stannard(4) is that their results show that there are radiation-induced defect energy levels deeper than about E_c-0.3eV also effective in trapping carriers, but they(3,4) are not able to locate the levels because the material becomes intrinsic and puts a limit on the region of the forbidden gap which can be studied using Hall Effect as the probe. By examining all results given here in Figures 3 - 8, we can see that deep levels are present and are important in trapping carriers, and are located in the forbidden gap as determined by extrinsic photoconductivity from these levels.

Although not given in the figures we have observed strong effects of both radiation and lithium doping concentration on the band edge. These results in the 1.1 to $\approx$1.25eV range are currently being analyzed and will be reported on later. Essentially, what we observe is that the band edge becomes less sharply defined and in fact appears to close i.e., a decrease in the forbidden gap energy results from the radiation and lithium doping effects.

In Table I we give a summary of the irradiated samples studied up to the current status of annealing. In all cases we see that the sample resistance increases after annealing as shown by the resistance measurements made at 78°K and at 300°K. Also given in Table I are the fluence and lithium concentration.

Before concluding we can extract some significant trends in the energy levels observed in the irradiated samples. First and foremost it is very difficult to quote energy levels from the results in Figures 3 and 4 since we do not have pronounced well defined energy levels appearing in the spectrum. In many of the spectra we do observe a good indication for a photoconductivity level at E_C-0.64eV, or it may be a level 0.50ev below the conduction band. In any case this level may be characteristic of Li doping since we have not observed a level in this energy position in irradiated Si containing other impurities (P, As, In). In many of the spectra we find strong evidence for a level near E_C-0.39eV (see Figures 5, 6, and 8) which might be associated with the doubly negative charge state of the divacancy energy level as reported by Kalma and Corelli[1]. However, in no sample do we have clear evidence for the presence of a level at E_C-0.54eV which was identified[1] with the singly negative charge state of the divacancy by Kalma and Corelli[1].

Thus far our results show only a minimal correlation from sample to sample relative to the presence of the same energy levels. Perhaps the most significant correlations are the presence of a level near E_C-0.64eV for all samples, the level near E_c-0.39eV (which appears to be shifted to E_c-0.34eV in some of the samples), and PC due to a level or levels lying within $\approx$ 0.2 to 0.3eV of the bottom of the conduction band.

We shall have more possibilities to make correlations of energy levels when experiments currently underway are completed. We must also extend our measurements to lower energies, i.e., $\approx E_c$-0.10eV (if possible) to determine if A-center defects ($\approx E_c$-0.18eV) can be detected.

TABLE I

SAMPLE CHARACTERISTIES AND RESISTANCE BEFORE AND AFTER IRRADIATION AND ANNEALING

		JPL-17	JPL-11	JPL-69
After Li	Resistance @ 78°K	1.5 Ω	1.2 Ω	4 Ω
Diffusion	Resistance @ 300°K	0.5 Ω	0.4 Ω	12 Ω
After	Resistance @ 78°K	8.0×10^7 Ω	2.0×10^8 Ω	2.0×10^8 Ω
Irradiation	Resistance @ 300°K	5.2 Ω	2.1 Ω	950×10^3 Ω
After 15 minutes	Resistance @ 78°K	8.0×10^{11} Ω	3.2×10^{11} Ω	2.0×10^8 Ω
@ 100°C	Resistance @ 300°K	3.4×10^3 Ω	3.2×10^3 Ω	0.5×10^6 Ω
Fluence				
e/cm^2		6.3×10^{17}	6.0×10^{17}	2.0×10^{17}
Li				
cm^{-3}		2.0×10^{17}	9.0×10^{16}	9.0×10^{15}
Crystal Growth		CG	CG	FZ

PLANS FOR NEXT FOUR MONTHS

1. Perform cold temperature (80°K) irradiation ($\lesssim$ 3 MeV electrons) and measure photoconductivity and if time permits infrared spectra with annealing up to $\sim$ 400°K.

2. Continue annealing present samples up to $\sim$ 400°C and measure PC.

3. Extend PC measurements to longer wavelength $E < 0.2$eV to check abrupt rise in spectra.

REFERENCES

(1) A. H. Kalma, and J. C. Corelli, Phys. Rev. 173, 734 (1968).

(2) R. C. Young and J. C. Corelli, Report to Air Force Cambridge Research Laboratories, April 1970, (unpublished), Rensselaer Polytechnic Institute.

(3) G. Brucker, T. Faith, J. Corra and A. Holmes-Siedle, Third Quarterly Report, JPL Contract 952555, prepared by RCA and issued 10 April 1970.

(4) J. Stannard, Proceedings of the Conference of Effects of Lithium Doping on Silicon Solar Cells, Jet Propulsion Laboratory, Pasadena, California, May 9, 1969.

FIGURE CAPTIONS

Figure 1) Cryostat tail piece showing details of sample holder and how the infrared light is incident on the sample.

Figure 2) Cryostat tail piece showing in detail how the electron beam is allowed to strike the sample.

Figure 3) Relative photoconductivity $\frac{\Delta\sigma}{\sigma\Omega}$ vs. energy of light for an unirradiated CG silicon doped to a lithium concentration of $1.2 \times 10^{16} cm^{-3}$. The worst energy resolution ΔE is shown on the figure. (Sample JPL #30).

Figure 4) Relative photoconductivity ($\frac{\Delta\sigma}{\sigma\Omega}$) vs. energy of light for a CG silicon sample doped to a lithium concentration of $9 \times 10^{16} cm^{-3}$ after 1.5MeV electron irradiation to a fluence of $6 \times 10^{17} cm^{-2}$. (Sample JPL #11).

Figure 5) Relative photoconductivity $\frac{\Delta\sigma}{\sigma\Omega}$ vs. energy of light for sample JPL-11 (shown in Figure 4) after 15 minutes annealing at 100^{o}C.

Figure 6) Relative photoconductivity ($\frac{\Delta\sigma}{\sigma\Omega}$) vs. energy of light for a floating zone silicon sample doped to a lithium concentration of $9 \times 10^{15} cm^{-3}$ after 1.5MeV electron irradiation to a fluence of $2 \times 10^{17} cm^{-2}$ (sample JPL-69).

Figure 7) Relative photoconductivity ($\frac{\Delta\sigma}{\sigma\Omega}$) vs. energy of light for the sample JPL-69 (shown in Figure 6) after 15 minutes annealing at 110^{o}C.

Figure 8) Relative photoconductivity ($\frac{\Delta\sigma}{\sigma\Omega}$) vs. energy of light for a crucible grown silicon sample doped to a lithium concentration of $2 \times 10^{17} cm^{-3}$ after 1.5MeV electron irradiation to a fluence of $6.3 \times 10^{17} e/cm^2$. (Sample JPL #17)

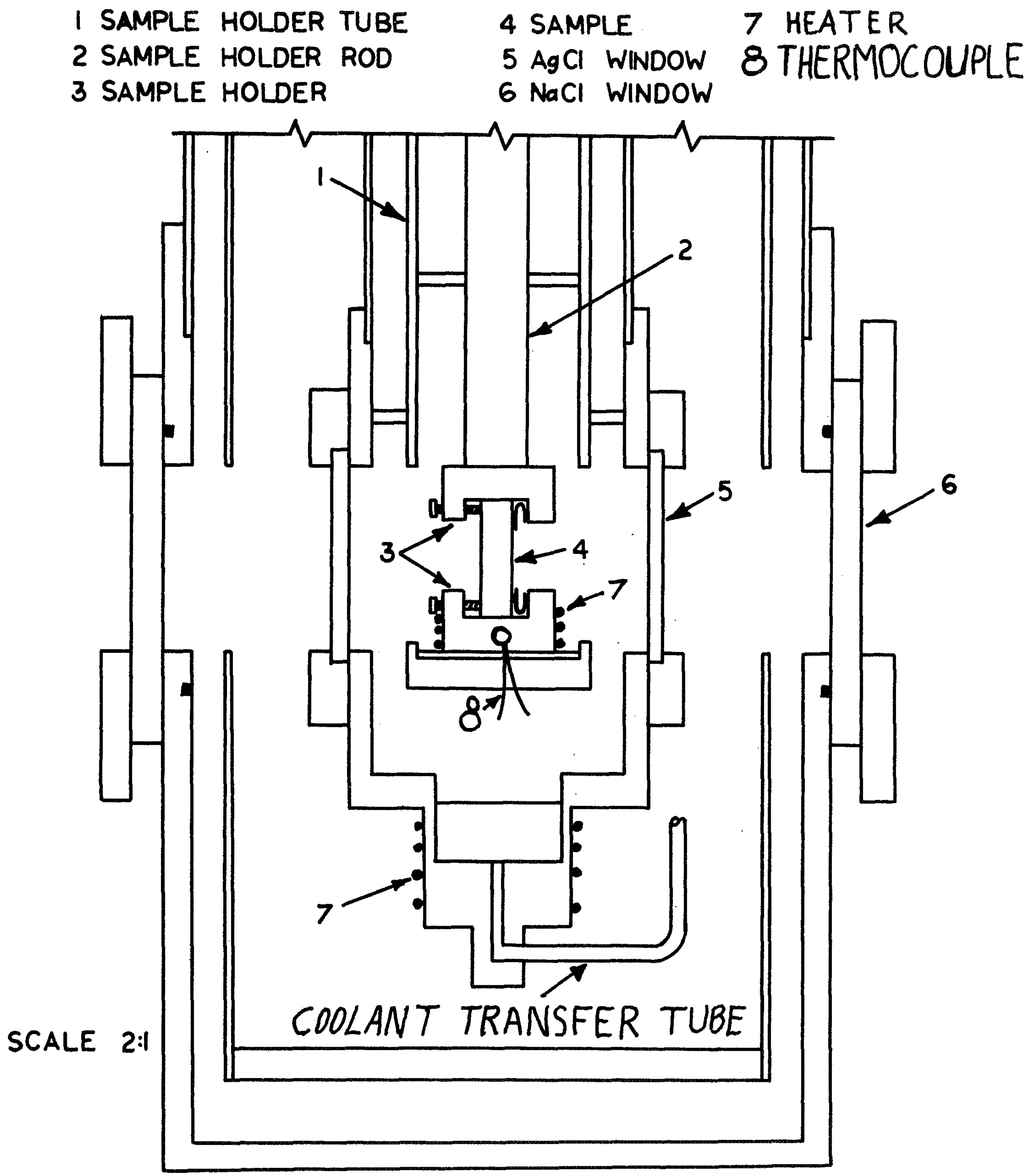

FIG 1. TAIL PIECE OF IRRADIATION CRYOSTAT

1. 0.0005" KAPTON FILM
2. 0.003" ALUMINUM FOIL
3. 0.010" ALUMINUM FOIL
4. 0.010" ALUMINUM FOIL
5. SAMPLE

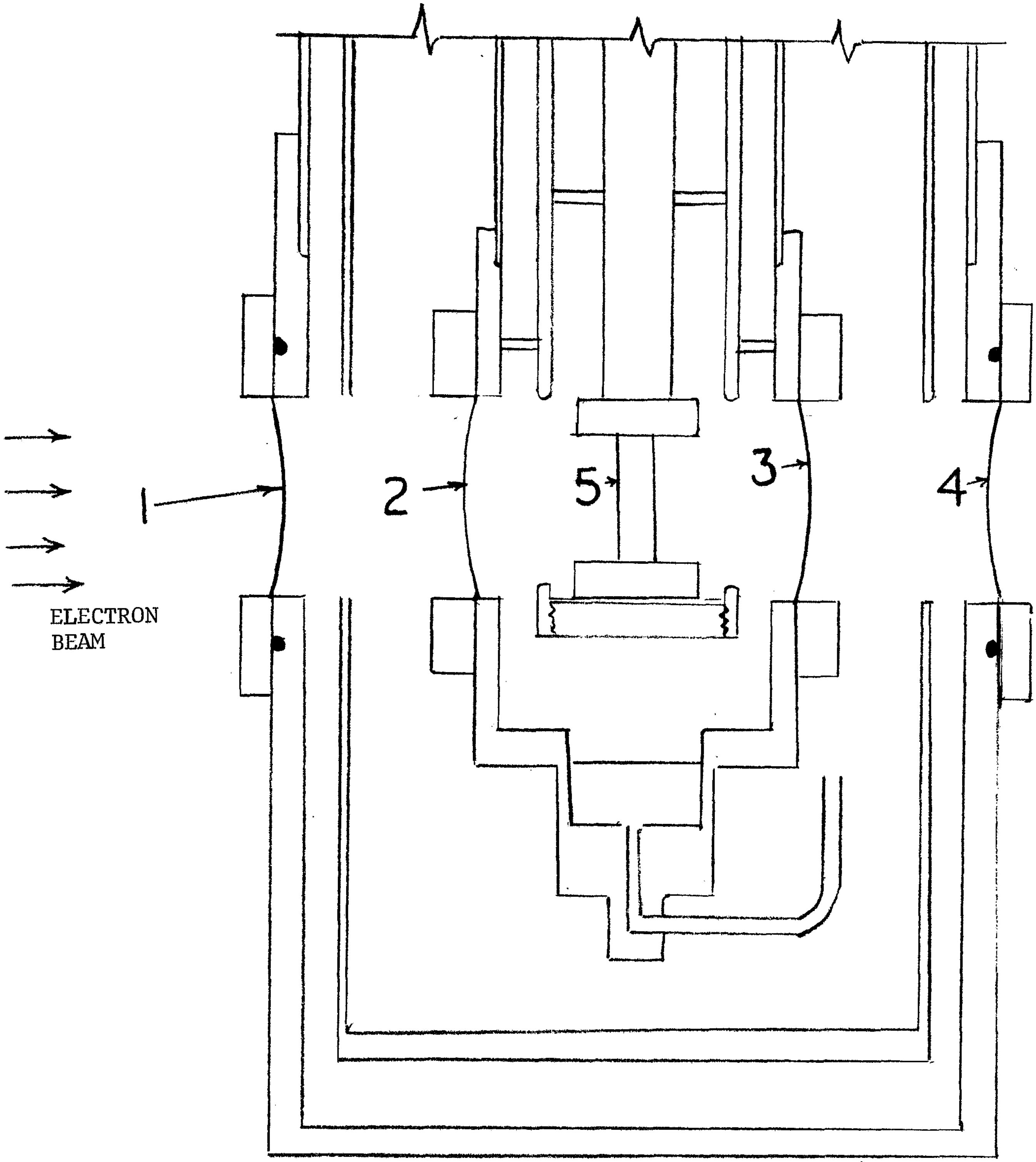

FIG. 2 CRYOSTAT TAIL PIECE SHOWING HOW ELECTRON BEAM STRIKES SAMPLE

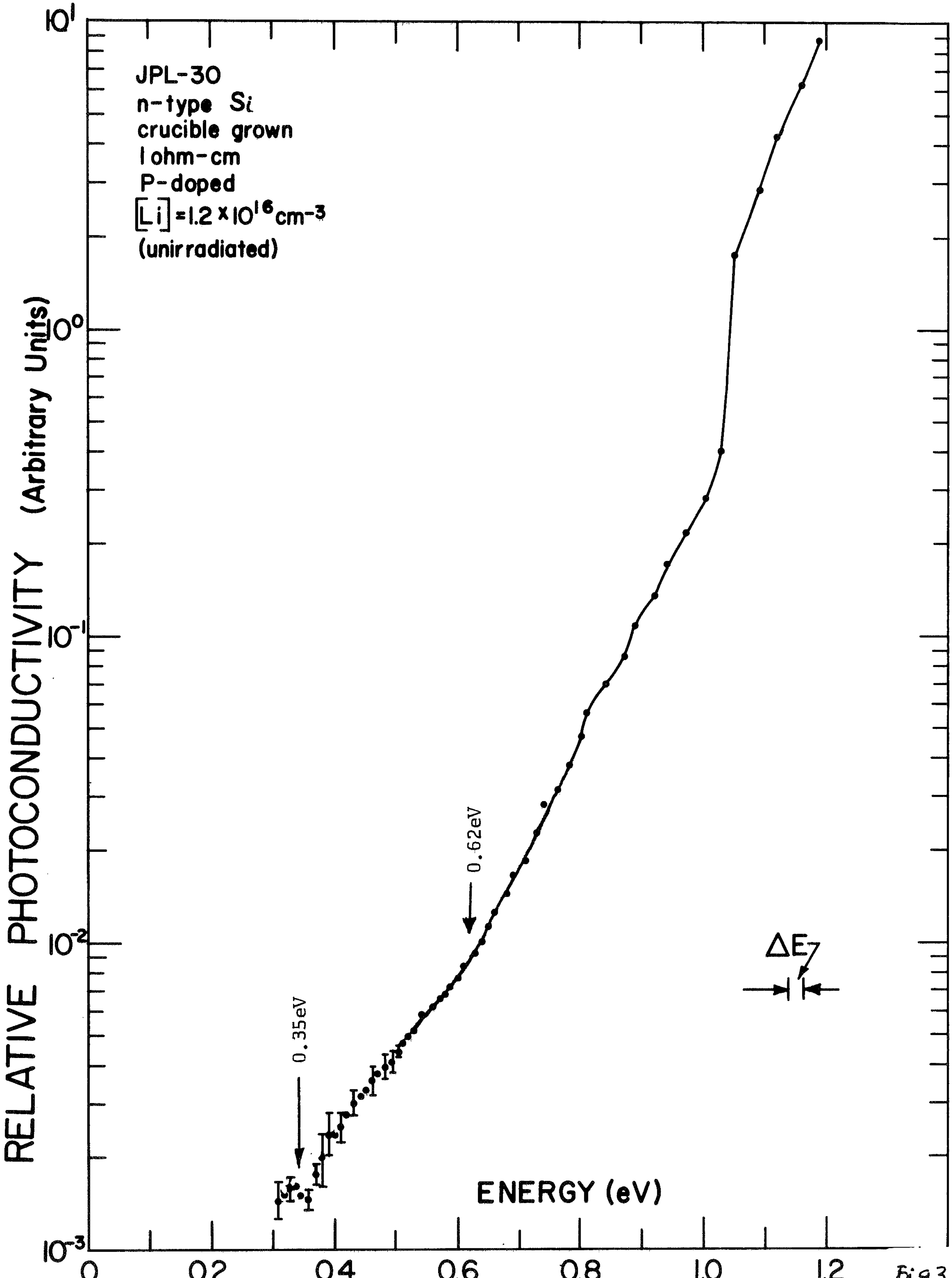
JPL-30
n-type Si
crucible grown
1 ohm-cm
P-doped
[Li] = 1.2 x 10^16 cm^-3
(unirradiated)
RELATIVE PHOTOCONDUCTIVITY (Arbitrary Units)
ENERGY (eV)
0.35eV
0.62eV
ΔE7
10^1
10^0
10^-1
10^-2
10^-3
0
0.2
0.4
0.6
0.8
1.0
1.2
Fig 3

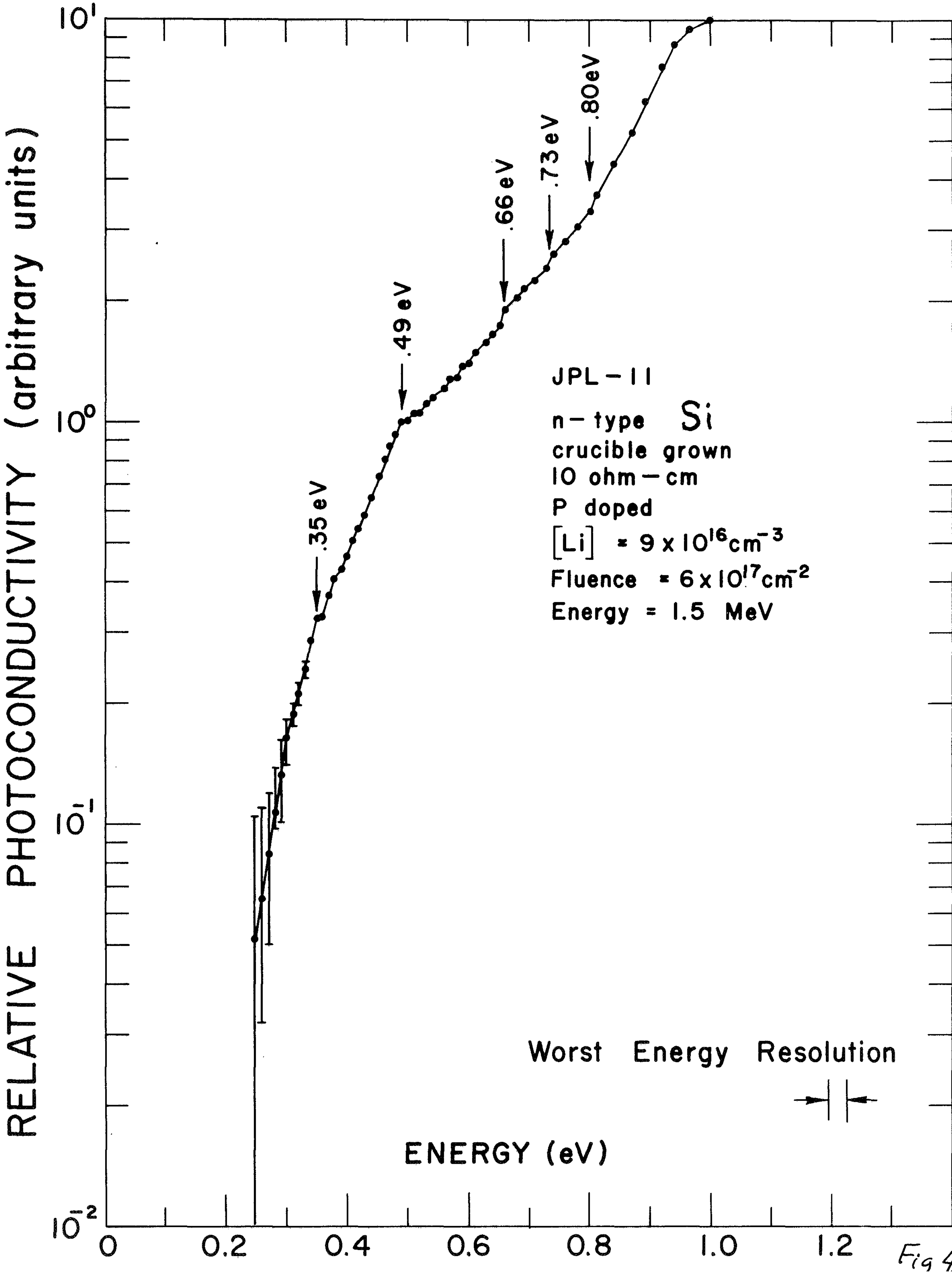

RELATIVE PHOTOCONDUCTIVITY (arbitrary units)
10¹
10⁰
10⁻¹
10⁻²
ENERGY (eV)
0
0.2
0.4
0.6
0.8
1.0
1.2
.35 eV
.49 eV
.66 eV
.73 eV
.80 eV
JPL - 11
n-type Si
crucible grown
10 ohm-cm
P doped
[Li] = 9 x 10¹⁶ cm⁻³
Fluence = 6 x 10¹⁷ cm⁻²
Energy = 1.5 MeV
Worst Energy Resolution

Fig 4).

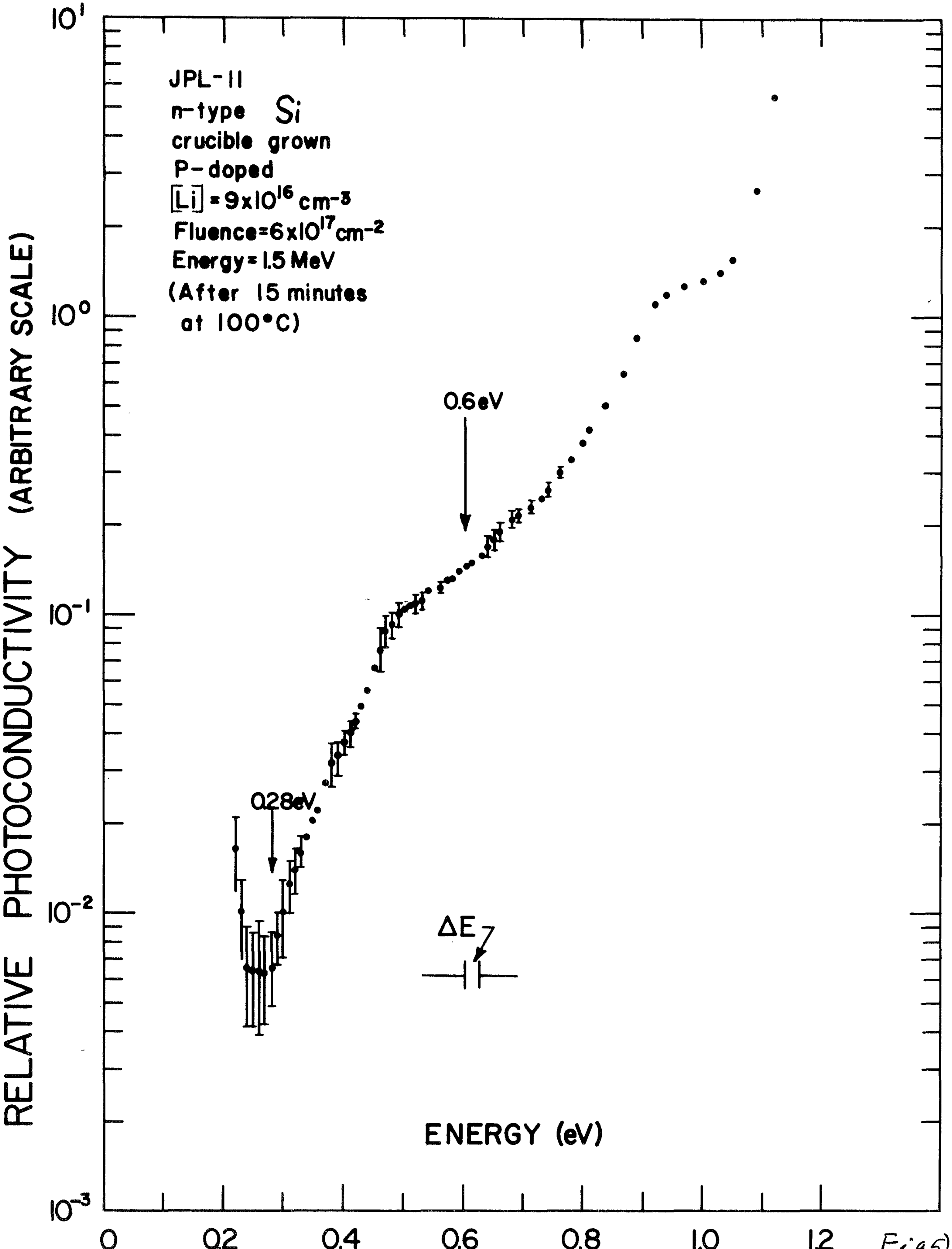

JPL-11
n-type Si
crucible grown
P-doped
[Li] = 9x10^16 cm^-3
Fluence=6x10^17 cm^-2
Energy= 1.5 MeV
(After 15 minutes
at 100°C)
0.6eV
0.28eV
ΔE
RELATIVE PHOTOCONDUCTIVITY (ARBITRARY SCALE)
ENERGY (eV)
10^1
10^0
10^-1
10^-2
10^-3
0
0.2
0.4
0.6
0.8
1.0
1.2

Fig 5)

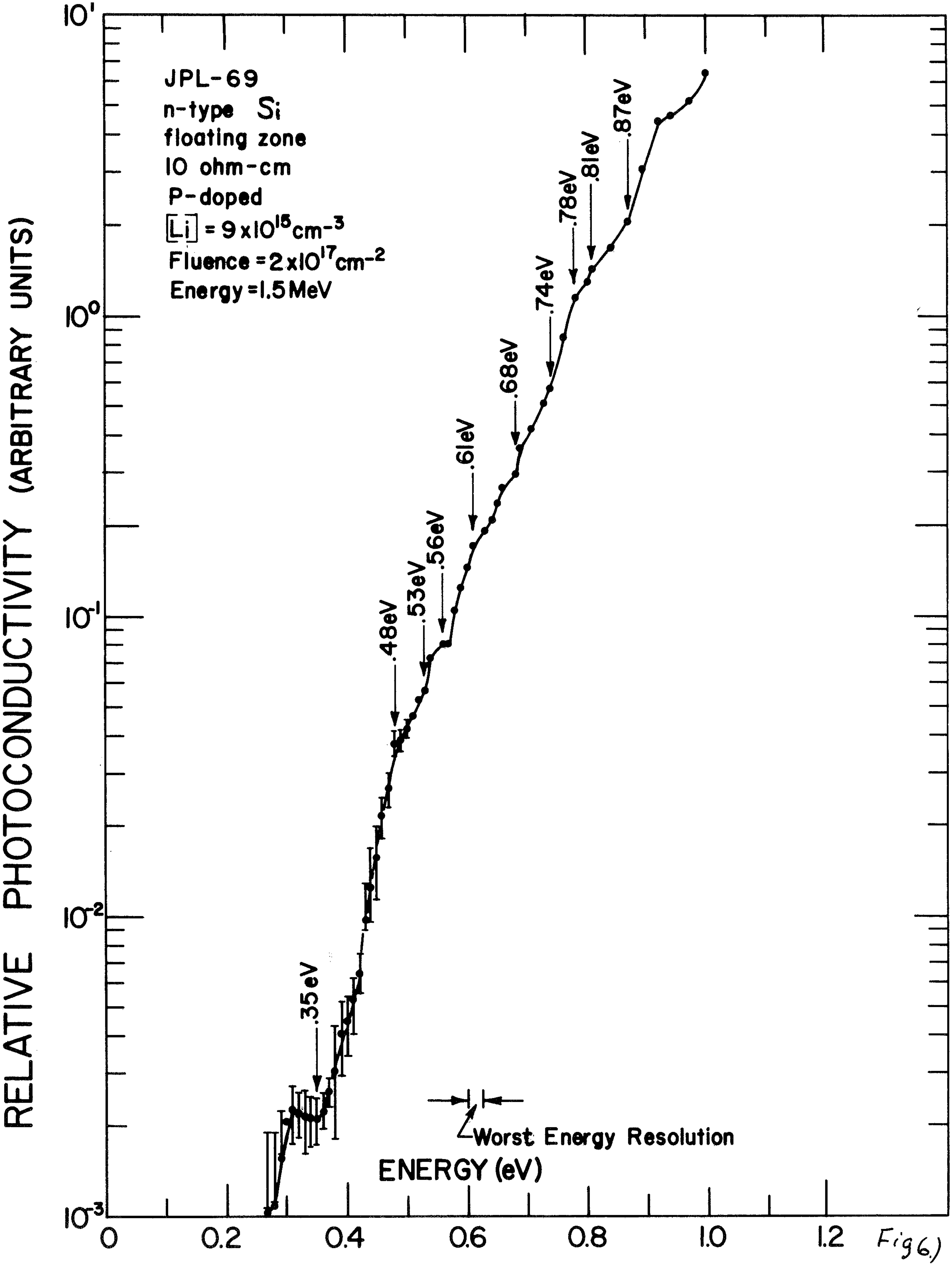
JPL-69
n-type Si
floating zone
10 ohm-cm
P-doped
[Li] = 9x10^15 cm^-3
Fluence = 2x10^17 cm^-2
Energy = 1.5 MeV
RELATIVE PHOTOCONDUCTIVITY (ARBITRARY UNITS)
10^1
10^0
10^-1
10^-2
10^-3
.35eV
.48eV
.53eV
.56eV
.61eV
.68eV
.74eV
.78eV
.81eV
.87eV
Worst Energy Resolution
ENERGY (eV)
0
0.2
0.4
0.6
0.8
1.0
1.2
Fig 6.)

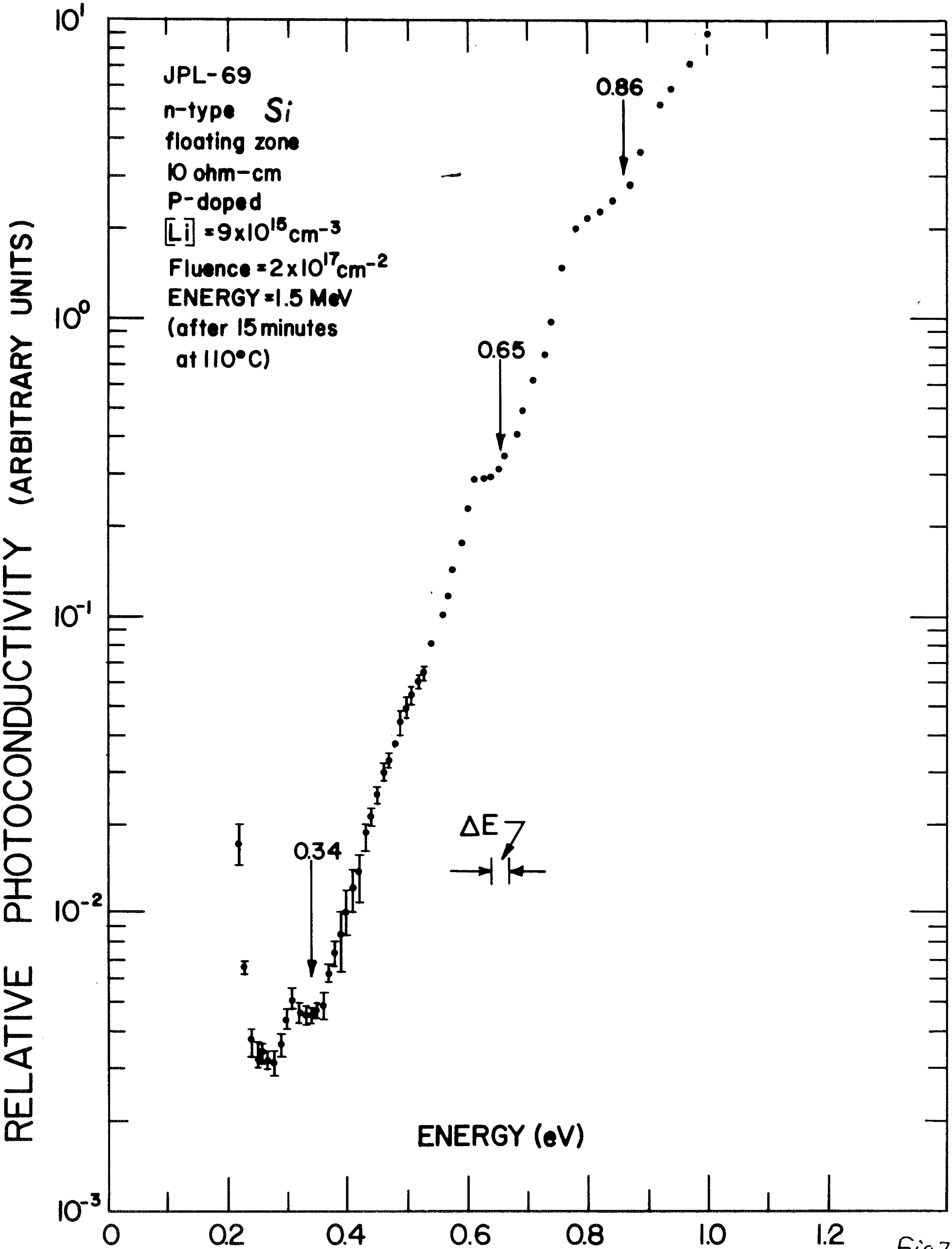

JPL-69
n-type Si
floating zone
10 ohm-cm
P-doped
[Li] = 9x10^15 cm^-3
Fluence = 2x10^17 cm^-2
ENERGY = 1.5 MeV
(after 15 minutes
at 110°C)
0.86
0.65
0.34
ΔE
RELATIVE PHOTOCONDUCTIVITY (ARBITRARY UNITS)
ENERGY (eV)
10^1
10^0
10^-1
10^-2
10^-3
0
0.2
0.4
0.6
0.8
1.0
1.2

Fig 7)

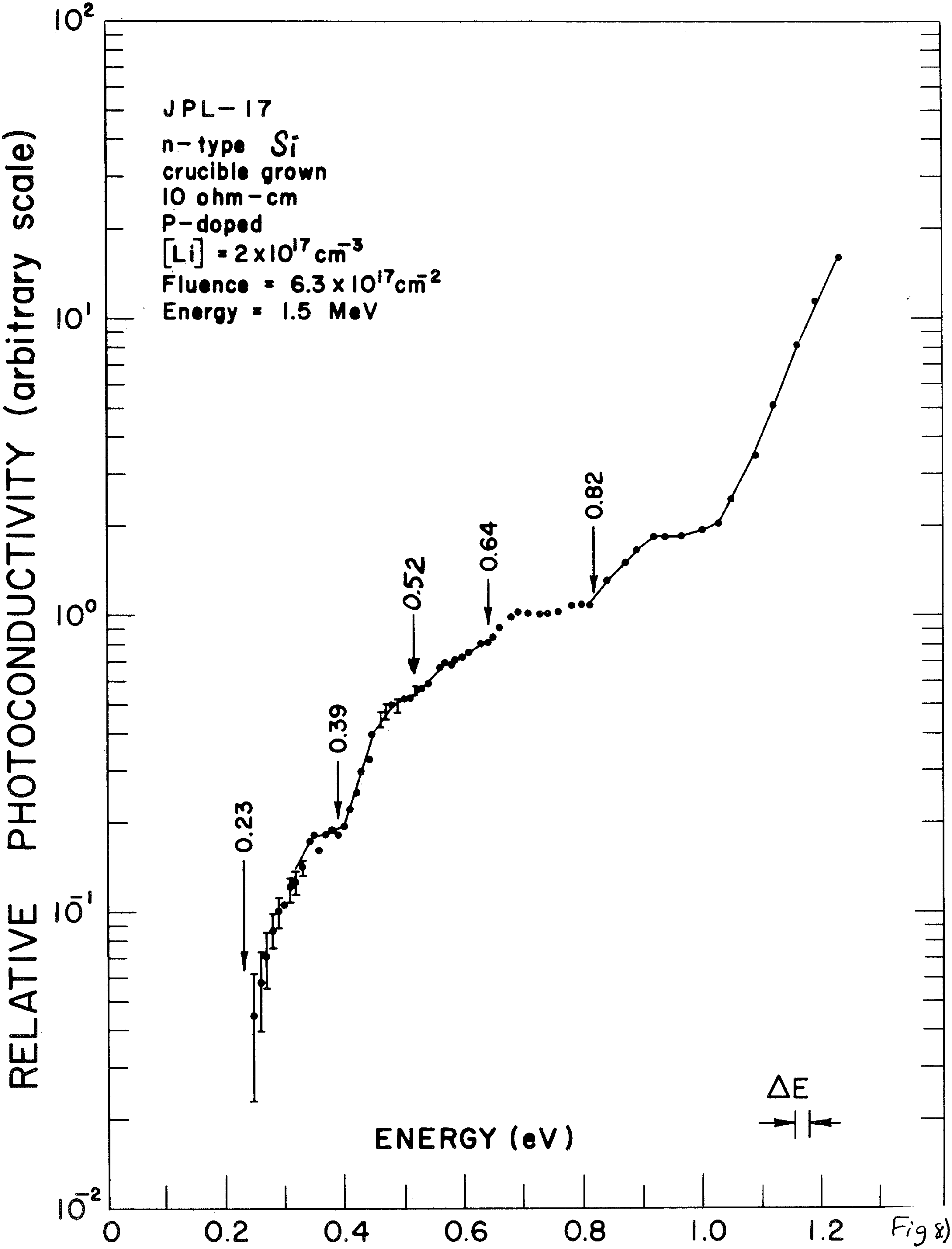

JPL-17
n-type Si
crucible grown
10 ohm-cm
P-doped
[Li] = 2 x 10^17 cm^-3
Fluence = 6.3 x 10^17 cm^-2
Energy = 1.5 MeV
RELATIVE PHOTOCONDUCTIVITY (arbitrary scale)
ENERGY (eV)
0.23
0.39
0.52
0.64
0.82
ΔE
10^2
10^1
10^0
10^-1
10^-2
0
0.2
0.4
0.6
0.8
1.0
1.2

Fig 8)